

MicroBooNE low-energy excess signal prediction from unfolding MiniBooNE Monte-Carlo and data

MICROBOONE-NOTE-1043-PUB

MicroBooNE Collaboration,
microboone_info@fnal.gov

July 7, 2018

One of the primary goals of MicroBooNE is to address the existence and underlying source of the MiniBooNE observed Low Energy Excess (LEE). The MiniBooNE LEE is the observation of an anomalous excess of ν_e charged current quasi-elastic-like events in the Booster Neutrino Beam at Fermilab. The true origin of those events could be attributed to either single electrons or single photons produced in the MiniBooNE Cherenkov detector, as the experiment lacked the ability to distinguish between the two. Using the ability of liquid argon time projection chambers to perform electron/photon separation, MicroBooNE aims to search for this excess in two exclusive channels: single photon and single electron. However before addressing either hypothesis the MiniBooNE LEE must be explicitly modeled in MicroBooNE. This requires that the MiniBooNE detector response, event reconstruction, selection and their collective effects be removed before mapping the observable excess to MicroBooNE. This note describes this “unfolding process,” and provides the end results of the true unfolded distributions for two well motivated LEE hypotheses: (a) electrons from an increased intrinsic ν_e charged current event rate and (b) single photons due to neutrino neutral current Δ production with subsequent radiative decay.

1 Introduction

The MiniBooNE experiment searched for $\nu_\mu \rightarrow \nu_e$ oscillations by looking for an excess in electron-like events in the Booster Neutrino Beam (BNB) at Fermilab [1]. This was primarily motivated by a prior $\bar{\nu}_\mu \rightarrow \bar{\nu}_e$ -like signal at the LSND experiment [2], which although using a different neutrino source at a different baseline, had a similar L/E_ν as MiniBooNE. This allowed MiniBooNE to probe oscillations at the same Δm^2 as suggested by LSND, interpreted as light sterile neutrino induced oscillations [3, 4]. Although MiniBooNE did indeed observe a significant excess of ν_e charged current quasi elastic (CCQE)-like events, the majority of the excess was reconstructed at a lower energy than generally expected if the 1 eV² oscillation hypothesis of LSND was indeed their true origin, instead favouring smaller mass-splittings and much larger mixing angles than the LSND anomaly. This “low energy excess” (LEE) is shown in Fig. 1.

Dispite the slight tension in parameter space between LSND and MiniBooNE sterile explanations, the most widely discussed explanation of the LEE is still ν_μ in the BNB oscillating into ν_e at a high Δm^2 (i.e. the light sterile neutrino oscillation hypothesis), followed by the ν_e interacting in the detector through CCQE scattering and producing a single electron (plus hadronic recoils not typically reconstructible in MiniBooNE). However, due to MiniBooNE being a mineral oil ($C_N H_{2N}$) Cherenkov detector, and consequently its inability to differentiate electromagnetic (EM) shower Cherenkov rings that originate from either an electron or a photon, the MiniBooNE LEE could also be interpreted as an excess of single photon events rather than single electron events, or even some combination of the two. As can be seen in Fig. 1, photons coming from neutral current (NC) π^0 events and NC radiative $\Delta \rightarrow N\gamma$ decay events, where N is a proton or neutron, are the largest background at the low energy region where the excess is present.

The MicroBooNE experiment[5] is a liquid argon time projection chamber (LArTPC) detector sitting in the same neutrino beam at a similar baseline as the MiniBooNE experiment. Using a combination of calorimetric energy deposition studies of the beginning of an EM shower (dE/dx) as well as observation of a photon-conversion gap relative to an event vertex (e.g. if an associated track is also visible), MicroBooNE can separate out photons and electrons and thus discern the origin of the MiniBooNE LEE.

In order to test any hypothesis of the LEE origin at MicroBooNE one needs a concrete model. For the sterile neutrino hypothesis, the model is based purely on BNB flux predictions from first principles and “3+1” neutrino oscillation theory [3], followed by MicroBooNE cross-section and detector Monte Carlo. If one wants to test more generic non-oscillation hypothesis, however, the effects of the MiniBooNE detector, reconstruction, and event selection must be “removed” or “unfolded” in order to estimate the true underlying excess prediction before generating a corresponding signal in the MicroBooNE Monte Carlo for further testing. This still must be performed under some concrete assumptions about the nature of the excess; i.e. a completely model-independent MiniBooNE LEE signal prediction is not possible to arrive at, since, depending on the underlying hypothesis, the unfolding of detector effects can lead to drastically different truth information.

In order to perform this unfolding for a variety of model hypothesis the full MiniBooNE Monte Carlo simulation that went into the CCQE analysis, both before and after analysis selection, as well as the observed data is required at an event-by-event level, rather than the binned final histogram as was in the public release, https://www-boone.fnal.gov/for_physicists/data_release/. To this end, the MiniBooNE collaboration graciously granted us access to their Monte Carlo and data used in the 6.46E20 POT neutrino mode analysis.

Currently, there are several ongoing analysis efforts in MicroBooNE to search for a LEE [6, 7, 8, 9], utilizing multiple and complementary reconstruction frameworks. For each and all of those efforts, a common and accurate LEE signal prediction is necessary for a variety of purposes:

1. Analysis optimization: Reconstruction, particle identification, and event selection has to be developed and optimized for any given LEE signal hypothesis, and this optimization should aim to maximize

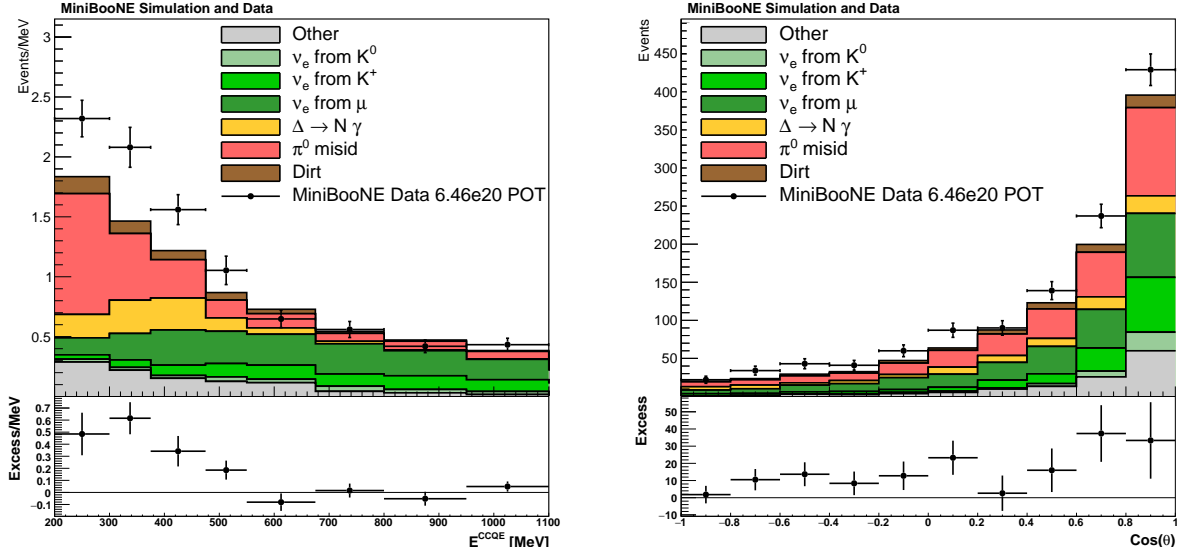


Figure 1: The MiniBooNE CCQE analysis results showing breakdown of the Monte Carlo simulation predicted backgrounds as well as data from the initial 6.46E20 protons-on-target (POT) exposure in the neutrino-mode BNB. This figure is the same as in the MiniBooNE publications, but remade using their Monte Carlo simulation. The event spectra are binned in reconstructed neutrino energy assuming quasi-elastic scattering (E_{ν}^{QE}) (Left), and in cosine of the angle of the reconstructed EM shower relative to the beam axis (Right).

the significance of an observation consistent with a signal hypothesis relative to the background-only hypothesis. This requires that the analyzers compare the results of reconstruction, particle identification and event selection strategies for both signal and background samples, and that they also study limitations due to systematic effects on both samples.

2. Quantifying final sensitivity and measurement significance: Any LEE search must be characterized by its final sensitivity to a signal hypothesis. Furthermore, in the case of a positive (excess) result, an excess significance relative to a background-only prediction can be quantified without the need for an excess signal prediction; however, to quantify consistency of any observed excess with a given signal hypothesis, a signal simulation is needed. In addition, the significance of signal predictions relative to alternative signal hypotheses, and not just background-only predictions, is important for quantitative remarks on whether or not the (positive) data favors any particular signal interpretation over another. In the case of a null result, a signal simulation is needed in order to calculate the significance with which a given excess hypothesis is excluded.
3. Providing a meaningful physics statement: Following a LEE search the significance of any excess or lack thereof must be quantified, and the consequence of either result elaborated in terms of a particular physics hypothesis. For example, if a significant excess is observed, consistent with a particular hypothesis, one could further investigate whether the observed properties of the excess explicitly agree with given model predictions.
4. Allowing direct comparisons between independent analyses. In order to facilitate the direct comparison of results obtained in, for example, independent reconstruction and analysis selection schemes, one must ensure the underlying LEE signal hypothesis is the same in all analyses, for a given signal model. This is of particular importance in the event that there is disagreement in results when analyzed under different frameworks.

2 Unfolding Methodology

In translating the MiniBooNE observed excess, given as a function of reconstructed variables, to the MiniBooNE true (or “raw”) excess as a function of a specific truth-level variable, one must “unfold” the effects of finite resolution, efficiencies and other detector effects. In this unfolding, a map between a reconstructed variable (e.g. E_ν^{QE} , visible energy E_{visible} , or $\cos\theta$) *after* the MiniBooNE ν_e CCQE event selection is applied, to an underlying true variable (usually true neutrino energy, E_ν), is constructed. The resulting map or “response” matrix encapsulates not only the detector effects, but also the efficiencies of the particular CCQE selection cuts.

This act of “unfolding” is neither uniquely defined nor a well behaved process when taken at face value. The “folding” process usually entails loss of information, meaning that the inverse, unfolding, is an ill-posed task in which one inherently cannot recover the full original information. Furthermore, many, sometimes infinite, true solutions can be folded to produce statistically identical folded reconstructed spectra. These problems necessitate the use of regularization of the unfolding process, which are discussed further in later sections.

The detector effects, as well as analysis selection effects, are contained entirely in the response matrix¹. The response matrix, \mathcal{A} , can be intuitively understood as a conditional probability

$$\mathcal{A}_{i\alpha} = P(\text{Reconstructed in } i | \text{come from } \alpha), \quad (1)$$

which, under the assumption that \mathcal{A} is generated by Monte Carlo simulation (MC), is the probability that an event is reconstructed in bin- i , given that it was generated in truth bin- α ². It is not necessarily true that every true event is reconstructed somewhere; there may be inefficiencies in the system causing the “loss of events”, as would be expected in a physical detector. This event loss can be quantified by defining an efficiency

$$\sum_{i=0}^{n_r} \mathcal{A}_{i\alpha} = P(\text{Reconstructed somewhere} | \text{come from } \alpha) \equiv \epsilon_\alpha. \quad (2)$$

Mathematically, to unfold a measured spectrum, d , is to solve the system of n_r coupled linear equations given by

$$d = \mathcal{A}u \quad \Leftrightarrow \quad d_i = \sum_{\alpha=0}^{n_t} \mathcal{A}_{i\alpha} u_\alpha. \quad (3)$$

If the matrix \mathcal{A} is invertible, then the unfolding equation for the unfolded spectrum u can be explicitly solved,

$$u = \mathcal{A}^{-1}d \quad \Leftrightarrow \quad u_\alpha = \sum_{i=0}^{n_r} \mathcal{A}_{\alpha i}^{-1} d_i. \quad (4)$$

To solve this explicitly, one may take the single value decomposition (SVD) of the matrix \mathcal{A} ,

$$\mathcal{A} = OSV^T, \quad (5)$$

where O is an orthogonal $n_r \times n_r$ matrix, V is an orthogonal $n_t \times n_t$ matrix, and S is an $n_r \times n_t$ diagonal matrix containing zero(es) or positive elements. Any real $n_r \times n_t$ can be decomposed in this way. The diagonal elements of S , labeled $S_{ii} \equiv s_i$, are called the singular values of the response matrix A . One can

¹Often referred to as a smearing or migration matrix in the literature.

²By convention in this note, Latin indices ($i, j, k..$) run over reconstructed variables and have dimension n_r , and Greek indices ($\alpha, \beta, \gamma..$) run over truth variables of dimension n_t .

always assume that s_i will form a decreasing sequence, as one can swap columns of O and V as long as one swaps the corresponding singular values, with no change on the response matrix \mathcal{A} .

The SVD can be used to rotate the data, d_i , and the unfolded truth, u_α , such that new rotated vectors can be defined,

$$y \equiv V^T u \quad , \quad b \equiv O^T d. \quad (6)$$

In this basis, one can rewrite the system of coupled linear equations that make up $d = \mathcal{A}u$ as $Sy = b$, which is now a system of *decoupled independent linear equations*, as S is diagonal by definition, greatly simplifying the problem. Solving this explicitly gives $y_\alpha = \delta_{i\alpha} \frac{b_i}{s_i}$, where $S_{ij}^{-1} = 1/s_i$ for $i = j$ and zero otherwise. To obtain the true underlying unfolded spectra, this can then be rotated back

$$u_\alpha = \sum_{k=0}^{n_r} \sum_{j=0}^{n_r} V_{\alpha k} O_{kj}^T \left[\frac{d_j}{s_k} \right]. \quad (7)$$

After writing our unfolded spectrum in this way, a problem is immediately highlighted. If any singular values are zero (0), then the unfolding is not defined. This is well known from linear algebra, since, if a matrix has a zero (0) singular value, it is degenerate and its inverse does not exist. However, the scenario that any singular values are small in comparison to the observed data, is equally ill-defined, as then that element contributes hugely to the unfolded spectra. Furthermore, small, statistically insignificant fluctuations in d_j are amplified by the presence of a small, non-zero singular value, up to the point the value of d_j/s_k is essentially arbitrary. This problem can be so dramatic that small deviations of as little as one (1) event in one (1) bin can lead to unrecognizably different unfolded solutions. The effect of this is to produce rapidly varying solutions, often with unphysical, negative numbers of events, whose covariance matrix shows bin-to-bin differences of very large magnitude.

2.1 Unfolding Algorithms

The smearing and loss of events through inefficiencies that are modeled by the response matrix inherently contain a loss of information. As such, many possible combinations of truth level events that are very different might “fold” to very similar reconstructed spectra. Any function or algorithm that pertains to reverse this via some unfolding acts similarly to a non-injective function, whose inverse is not well defined.

Instead of directly inverting the response matrix, the problem of unfolding can be rephrased as finding the solution that minimizes the least squares problem

$$(\mathcal{A}u - d)^T D^{-1} (\mathcal{A}u - d) = \min. \quad (8)$$

The solution of this is known as a “maximum likelihood estimator”; directly inverting the response matrix is an example of this. As inverting the response matrix leads to a maximum likelihood estimator, and although the variance procuded via this method is huge, it can be shown that it is in fact the smallest possible covariance for all unbiased methods. More precisely, the variance of any unbiased estimator is bounded by the inverse of the Fisher information (the Cramer-rao bound [10, 11]) and the maximum likelihood estimator saturates that bound. Thus, any method constructed to reduce the variance will necessarily introduce a bias.

This introduces the concept of “regularization,” in which some small known bias (systematic uncertainty) is accepted in order to make a large improvement in variance (statistical uncertainty) in the final unfolded spectra. In practice, the regularization and problem can sometimes be constructed such that the introduced bias is almost negligible.

The primary method in this analysis is D’Agostini’s Iterative Bayesian Unfolding [12], although a second unrelated method, SVD Unfolding [13], has also been used as a cross-check. The primary methods for each algorithm are described briefly below, although for complete details please see references therein.

2.1.1 D’Agostini Iterative Method

The D’Agostini iterative approach [12] is a widely used method for unfolding both in the HEP community, as well as in optics, astronomy and audio-analysis fields where it is known as Richardson-Lucy deconvolution [14, 15]. It is motivated by Bayes theorem and requires an initial prior guess of the solution, u^0 , which is usually taken to be the Monte Carlo truth, t , or a flat distribution. It has the benefit of having a very easy and understandable algorithm in which the unfolding takes place.

This initial estimate u_α^0 , is then updated via the iterative algorithm utilizing Bayes theorem to derive the probabilities that a given reconstructed event originated in a particular true bin at iteration $k + 1$;

$$u_\alpha^{k+1} = \frac{1}{\epsilon_\alpha} \sum_{i=1}^{n_r} P(\text{Generated in } \alpha | \text{Reconstructed in } i), \quad (9)$$

$$= \frac{1}{\epsilon_\alpha} \sum_{i=1}^{n_r} \left[\frac{P(\text{Reconstructed in } i | \text{Generated in } \alpha) P(\text{Generated in } \alpha)}{P(\text{Reconstructed in } i)} \right], \quad (10)$$

$$= \frac{1}{\epsilon_\alpha} \sum_{i=1}^{n_r} \left[\frac{\mathcal{A}_{i\alpha} u_\alpha^k}{\sum_{\beta=1}^{n_t} \mathcal{A}_{i\beta} u_\beta^k} \right] d_i, \quad (11)$$

$$= \sum_{i=1}^{n_r} \mathcal{M}_{\alpha i}^k d_i \quad (12)$$

where in the equation 11 one uses the fact that $\mathcal{A}_{i\alpha}$ is the probability that an event generated in truth bin α is reconstructed in bin i , by construction, and in the last line, equation 12, the Bayesian “unfolding” matrix \mathcal{M}^k has been defined, which takes each iteration to the next. As can be seen, at each iteration step the prior probability is updated to the previous solution.

If one stops after one iteration, the result is maximally biased towards the initial estimate, often the Monte Carlo truth or a flat prior. However, if sufficient iterations are performed, the solution will eventually converge identically to the matrix inversion solution containing large variances and rapid statistical-driven oscillations [16]. Somewhere in between, the solution will contain some non-zero bias, but significantly smaller variance, thus the regularization parameter is the number of iterations undertaken. Note that, by construction, the number of events in the refolded spectrum for D’Agostini’s approach is identically that of the observed data, in this case the MiniBooNE excess. This is a very useful trait of D’Agostini’s method that is not guaranteed across other methods of unfolding, but ensures that all unfolded solutions will produce an excess of equal statistical significance to the observed data.

D’Agostini’s original method for computing the covariance matrix ignored the dependence of any given iteration on the previous iterations, underestimating the uncertainty if one makes more than one iteration, as was pointed out in [17]. One must calculate and update the error propagation matrix at each iteration,

$$\frac{\partial u_\alpha^{k+1}}{\partial d_i} = \mathcal{M}_{\alpha i} + \sum_{k=1}^{n_r} \mathcal{M}_{\alpha k} d_k \left(\frac{1}{u_\alpha^k} \frac{\partial u_\alpha^k}{\partial d_i} - \sum_{\beta=1}^{n_t} \frac{\epsilon_\beta}{u_\beta^k} \frac{\partial u_\beta^k}{\partial d_i} \mathcal{M}_{\beta k} \right). \quad (13)$$

This error propagation matrix can then be used to obtain the final covariance matrix on the unfolded distribution once your iteration has stopped,

$$U_{\alpha\beta} = \sum_{ij}^{n_r} \frac{\partial u_\alpha}{\partial d_i} D_{ij} \frac{\partial u_\beta}{\partial d_j}. \quad (14)$$

This takes into account the effect of systematic and statistical uncertainties and correlations in the measured data throughout the iterative unfolding. It does not, however, take into account the effect of

limited Monte Carlo statistics in constructing the response matrix, \mathcal{A} . Reference [18] provides more details on the construction of these error propagation formulae. In order to calculate the covariance matrix due to the underlying Monte Carlo, the error-propagation matrix for the unfolded solution (at iterative step k) due to the response matrix \mathcal{A} must be calculated, as that is where the MC uncertainty enters the solution. This matrix is given by

$$\frac{\partial u_\alpha^{k+1}}{\partial \mathcal{A}_{i\beta}} = \frac{1}{\epsilon_\alpha} \left(\frac{u_\alpha^k d_i}{\sum_\delta^{n_t} \mathcal{A}_{i\delta} u_\delta^k} - u_\alpha^{k+1} \right) \delta_{\alpha\beta} - \frac{u_\beta^k d_i}{\sum_\delta^{n_t} \mathcal{A}_{i\delta} u_\delta^k} \mathcal{M}_{\alpha i} + \quad (15)$$

$$\frac{u_\alpha^{k+1}}{u_\alpha^k} \frac{\partial u_\alpha^k}{\partial \mathcal{A}_{i\beta}} - \frac{\epsilon_\alpha}{u_\alpha^k} \sum_{l=1}^{n_r} \sum_{\gamma=1}^{n_t} d_l \mathcal{M}_{\alpha l} \mathcal{M}_{\gamma l} \frac{\partial u_\gamma^k}{\partial \mathcal{A}_{i\beta}}. \quad (16)$$

The final covariance matrix due to this term can be computed in the usual way,

$$U_{\alpha\beta} = \sum_{ij} \sum_{\gamma\delta} \frac{\partial u_\alpha}{\partial \mathcal{A}_{i\gamma}} V_{i\gamma, j\delta} \frac{\partial u_\beta}{\partial \mathcal{A}_{j\delta}}, \quad (17)$$

where a new higher-dimensional covariance matrix $V_{i\gamma, j\delta}$ has been introduced. This is the covariance between the $i\gamma$ 'th component of the 2D response matrix \mathcal{A} and the $j\delta$ 'th component. In practice this can be used to implement any statistical or systematic uncertainty that exists in the MiniBooNE Monte Carlo and ensure that they are propagated correctly onto the final unfolded example. This covariance matrix can then be added with the covariance matrix due to the uncertainty on the observed data as calculated above, to give a final covariance matrix for the full unfolded solution. One must be careful when including systematics on MiniBooNE's Monte Carlo to ensure you are not double counting in MicroBooNE's systematics also. This can be seen most clearly in the case of flux uncertainties as both MicroBooNE and MiniBooNE sit in the same beamline. As such until MicroBooNE's own systematic uncertainties are fully understood we are performing this analysis with only statistical uncertainty on the MiniBooNE Monte Carlo included in V , implemented by filling the higher dimensional "diagonal" of V with the corresponding statistical uncertainty of that bin.

2.1.2 SVD unfolding

The prescription outlined in Ref. [13] for SVD unfolding comes from studying the SVD of the response matrix \mathcal{A} . Although one can simply set a singular value to zero to remove it from the response matrix when folding, this method does not work for unfolding, as a matrix with even one zero singular value is a non-invertible degenerate matrix. As such, the SVD unfolding algorithm attempts to remove the effect of small singular values via a form of Tikhonov regularization [19].

In this form, the least-squares problem is modified to a form including a regularization scheme introduced with strength τ ,

$$(\mathcal{A}w - d)^{\text{Tr}} D^{-1} (\mathcal{A}w - d) + \tau (Ct)^{\text{Tr}} Cw = \min, \quad (18)$$

where C is a second-derivative "Curvature" matrix which favors results to be smooth and without sudden sharp steps. In addition to this regularization strength, a series of rotations and re-scalings are introduced, and the response matrix \mathcal{A} is recast as a "number-of-events" matrix in order to give more weights to entries which have higher statistics in the MiniBooNE Monte-Carlo and thus are better known. Reference [13] provides a detailed discussion of these rotations, as well as the exact derivation of the final solution for unfolded spectra; the result is quoted here for convenience. The effect of introducing τ means that the singular values shift and the exact inversion solution is replaced by the regularized solution

$$u_\alpha = t_\alpha \sum_{k=0}^{n_r} \sum_{\beta=1}^{n_t} C_{\alpha\beta}^{-1} V'_{\beta k} \left[\frac{\hat{d}_k s'_k}{s'_k{}^2 + \tau} \right], \quad (19)$$

where s' and V' now come from the SVD of $\hat{A}C^{-1} = O'S'(V')^T$, and \hat{A} is the rotated and scaled response matrix in a basis where the observed data, d , has been transformed to, \hat{d} , where it has a covariance matrix equal to a unit matrix, implying every entry in \hat{d} is uncorrelated and with the same uncertainty. The effect of non-zero τ can be seen immediately, effectively allowing for small and even zero singular values. Its effects are often likened to a cutoff for a low-pass filter, regularizing the singular effects of small s_j .

2.2 Choice of regularization parameter

By its very nature, folding in detector loss, energy resolution and cut efficiency, the folding procedure is an information lossy process. As such, many true spectra can fold to the same reconstructed spectra, and, inversely, given some observed reconstructed data spectrum, one can unfold it to a near infinite number of true underlying solutions which are statistically consistent with each other. As such there will always need to be a choice of one solution, or combination, over the others. In many cases one can invoke a prior physics requirement on the solution, e.g. a positive number of events; smooth, continuous distribution; etc. When the problem is phrased in terms of regularization, this choice corresponds to the choice of regularization strength. Central to choosing a regularization parameter is the concept followed in this analysis that the unfolded solution should be *“as accurate and precise a solution as possible, while remaining statistically consistent with the observed MiniBooNE data.”*

By this, a solution is required to satisfy the following criteria:

- Give as small a variance on unfolded spectra as possible: Minimize $\Sigma_{\alpha}^{n_t} U(\alpha, \alpha)$.
- Give zero (or consistent with zero) bias on the unfolded spectra: All $b_{\alpha}/\sqrt{B_{\alpha,\alpha}} \leq 1$, where B is the covariance matrix on the bias b .
- The MiniBooNE data be consistent with being a single experiment drawn from a distribution with expectation value equal to the refolded solution: $\chi^2(\delta, d)/ndof \leq 1$, where $\delta = Au$.

Given an infinite choice of regularization parameters, the above three conditions will give a single choice of regularization parameter. This was also motivated by the desire to avoid using an algorithm-specific method to choose the regularization, such as the SVD method of studying the singular values, as that way would necessitate different methods of choice in the cross-checks.

3 LEE Models

The tools described in the note can be applied to any hypothesis as to the origin of the LEE anomaly in order to arrive at a prediction at MicroBooNE. Two well-motivated LEE hypotheses are unfolded in this section: (a) electrons from an increased intrinsic ν_e charged current event rate and (b) single photons due to NC Δ production with subsequent radiative decay. Shown in Fig. 2 is the MiniBooNE excess stacked on top of each of the models' respective Monte Carlo components, after subtracting off the other background categories.

3.1 Electron-like Model: Enhanced intrinsic ν_e flux folded with CC cross-section

In this model it is assumed that the low energy excess is solely originating from an energy-dependent modification to the rate of intrinsic ν_e CC interactions. This is hypothesized to come from a combination of modified cross-section or flux which, although not greatly motivated from a theoretical stand point, it provides a simple, clean test-bed for the unfolding methods described above. This model has been the primary electron-like model for the MicroBooNE studies of the MiniBooNE LEE. Under this hypothesis, the MiniBooNE LEE can be reinterpreted as an excess of ν_e events above a background of intrinsic ν_e , as shown in Figure (2), after subtracting off the other non-intrinsic backgrounds. The true underlying spectrum is defined as the parent ν_e energy assuming that the neutrino interacted. The reconstructed variable is taken to

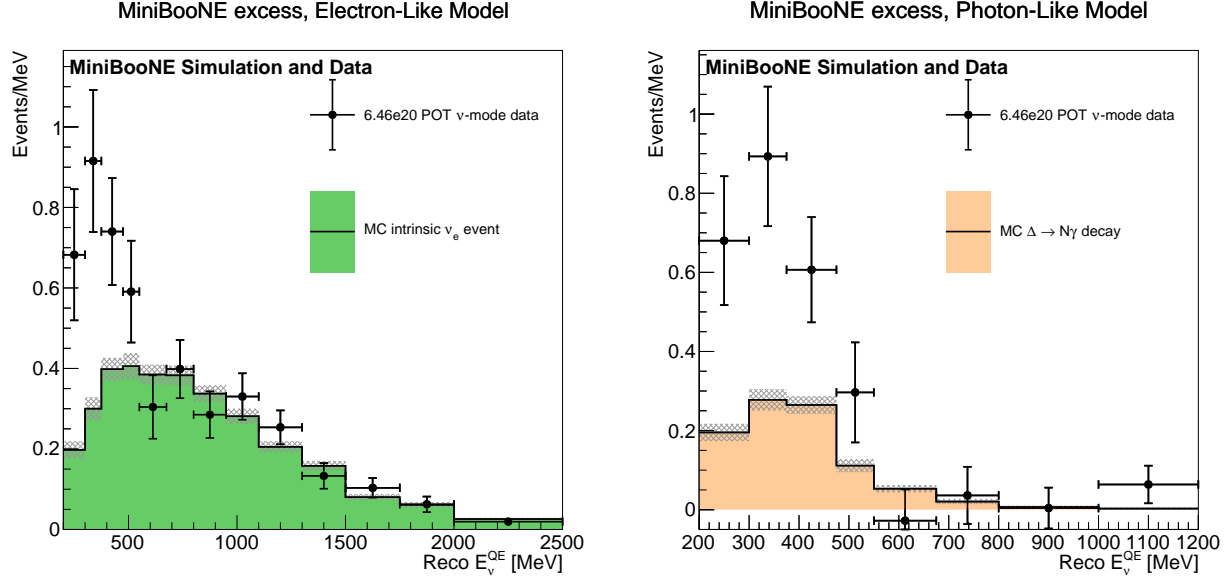


Figure 2: The MiniBooNE low-energy excess (observed MiniBooNE data minus total background prediction in MiniBooNE), compared to absolutely normalized MiniBooNE MC-predicted backgrounds originating from intrinsic ν_e only (left) and NC resonant Δ production and subsequent radiative decay (right), with the remaining backgrounds subtracted off. Error bars indicate full statistical uncertainties on observed data and MC statistical uncertainties are included as gray shaded region. It is the black data points that are the starting point for the unfolding. By assuming these explicit backgrounds (left/right) as the LEE source, the black points are then assumed to be the result of an increase in underlying green/tan spectra respectively. The unfolding procedure followed in this analysis aims at determining this increase quantitatively, as a function of some MC-truth variable for each exclusive source sample (intrinsic ν_e CC/NC $\Delta \rightarrow N\gamma$).

be the reconstructed neutrino energy assuming quasi elastic scattering, E_ν^{QE} , under the electron hypothesis, which is defined as

$$E_{QE} = \frac{m_N E_{\text{vis}} - \frac{1}{2} m_e^2}{m_N - E_{\text{vis}} + \sqrt{E_{\text{vis}}^2 - m_e^2} \cos \theta} \approx \frac{m_N E_{\text{vis}}}{m_N - E_{\text{vis}}(1 - \cos \theta)}, \quad (20)$$

where m_N is the mass of the struck nucleon, E_{vis} and $\cos \theta$ are the total visible energy and angle of a reconstructed electron-like Cherenkov cone. The true neutrino spectrum and reconstructed spectrum after CCQE event selection are provided in Fig. 3 alongside the associated response matrix \mathcal{A} and true neutrino energy dependent efficiency.

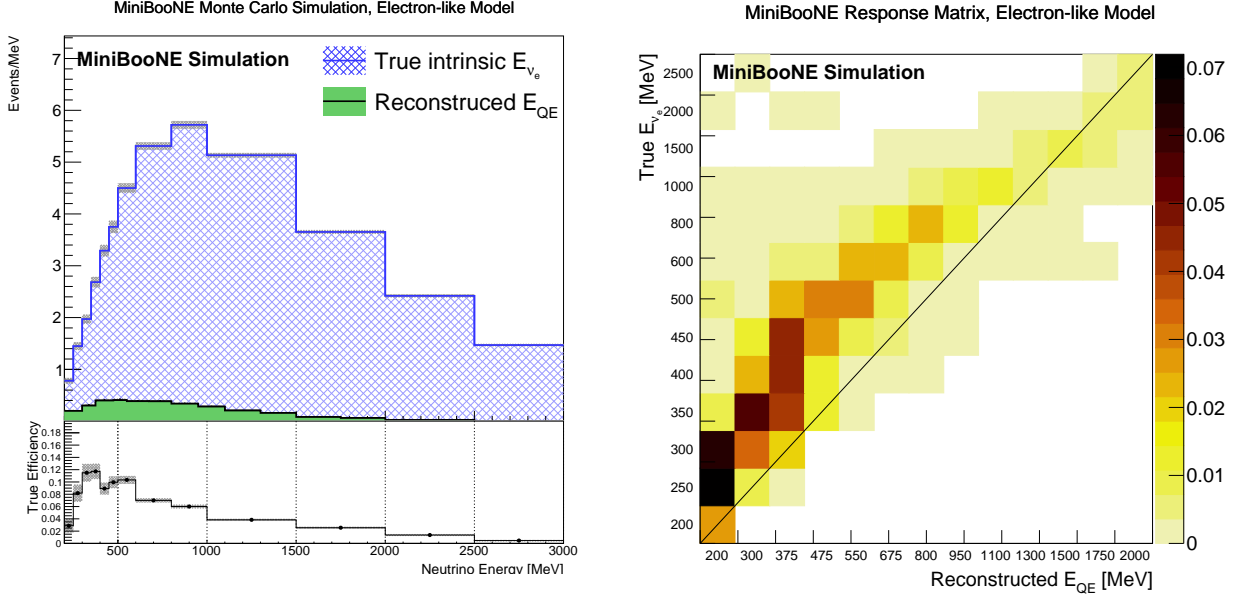


Figure 3: Left: True underlying intrinsic ν_e CC (t_α , in blue) and reconstructed ν_e CCQE event distributions in MiniBooNE, after reconstruction and MiniBooNE CCQE selection (r_i , in green), as functions of true neutrino energy E_ν and reconstructed E_ν^{QE} , respectively. Shown also is the combined detector, reconstruction, and ν_e CCQE selection efficiency in the bottom panel, as a function of true neutrino energy, E_ν . Note that below 200 MeV in true neutrino energy, no events pass the ν_e CCQE selection leading to a 0% efficiency. This means one cannot unfold to below 200 MeV in true neutrino energy. Right: The response matrix constructed such that it folds the Monte Carlo truth to Monte Carlo reconstructed variables as shown in the left, i.e. $r = At$. The z color scale represents the conditional probability.

4 Photon-like Model: Enhanced rate of NC Δ resonance with subsequent radiative decay

In this model it is assumed that the MiniBooNE LEE is solely due to an increased rate of resonant production of Δ 's (Δ^\pm or Δ^0) with subsequent radiative decay. The vast majority of events that pass the MiniBooNE CCQE selection cuts are NC Δ^0 events, with only 0.2% of radiative events being CC Δ^\pm production. Kinematically, resonant Δ production with subsequent radiative decay is very close spectrally to the LEE signal, as can be seen in Figure 1. Although constrained by electron scattering measurements, radiative decay of Δ 's from resonant scattering in the neutrino sector has never been directly measured and is the primary photon-like candidate that could explain the MiniBooNE LEE. The true underlying signal is defined as a function of the parent ν energy assuming NC Δ resonant interaction and subsequent radiative decay. The reconstructed variable is taken to be the reconstructed neutrino energy assuming CCQE scattering, E_ν^{QE} as defined above, taking the photon energy as the electron energy.

In Figure 4, the true and reconstructed spectra for NC $\Delta \rightarrow N\gamma$ in MiniBooNE are plotted alongside the associated response matrix mapping between them. As can be seen, the response matrix is highly off-diagonal, even more so than the case of the intrinsic ν_e CC model signal. In fact, the combined detector and CCQE selection efficiency is approximately energy independent, as seen in the bottom panel of the figure on the left. Thus, neutrinos of all energies that interact via NC scattering to produce a Δ are equally likely to produce a photon that is subsequently mis-identified as an electron in the MiniBooNE detector.

This would suggest that the unfolded spectrum should be closer to a flat normalization increase relative to the Monte Carlo predicted central value, which also follows from the fact that the Δ radiative sample is spectrally very close in shape to that of the observed LEE in MiniBooNE. In general, one can unfold into any true variable, not necessarily true neutrino energy. As a cross-check, the unfolding of the photon-like model has also been performed via true $\Delta \rightarrow N\gamma$ photon energy, yielding consistent results.

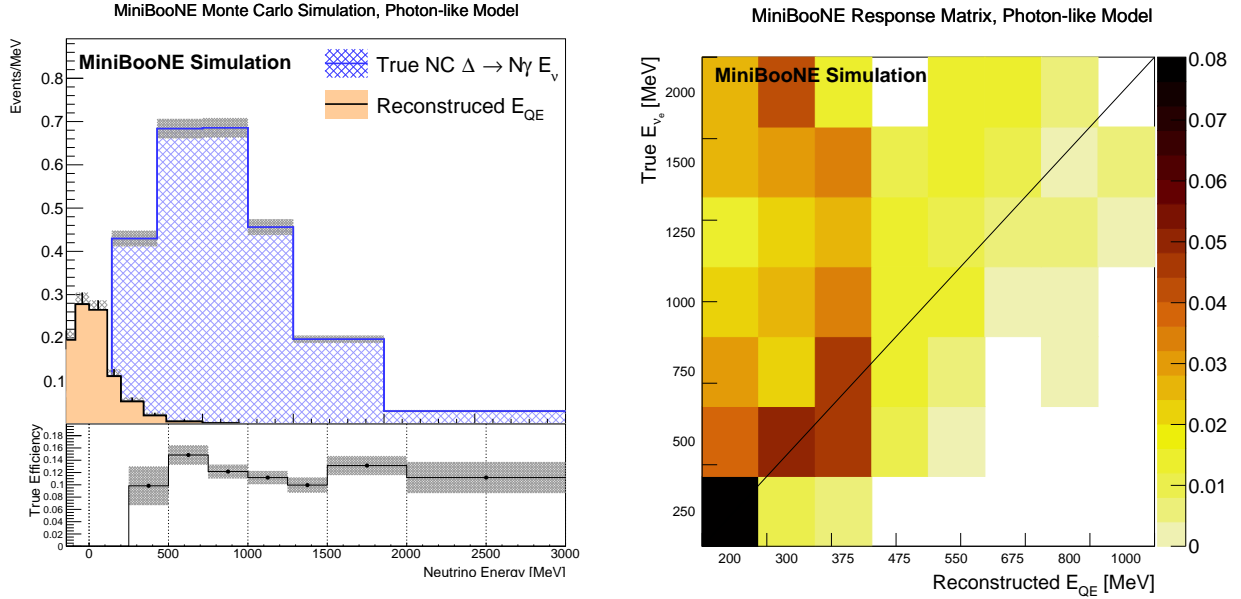


Figure 4: Left: True underlying NC $\Delta \rightarrow N\gamma$ resonant (t_α , in blue) and reconstructed NC $\Delta \rightarrow N\gamma$ event distributions in MiniBooNE, after reconstruction and MiniBooNE CCQE selection (r_i , in orange), as functions of true neutrino energy E_ν and reconstructed E_ν^{QE} , respectively. Shown also is the the combined detector, reconstruction, and ν_e CCQE selection efficiency in the bottom panel, as a function of true neutrino energy, E_ν . Right: The response matrix constructed such that it folds the Monte Carlo truth to Monte Carlo reconstructed variables as shown in the left, i.e. $r = At$. The z color scale represents the conditional probability.

5 Results and Conclusions

The results of unfolding both the electron-like and photon-like models are shown in Fig. 5. In the electron-like model case, one can see the strong energy dependence needed in the model, with little or no effect above 500 MeV, but almost a factor of 5 increase relative to the Monte Carlo central value required at lowest energies. This is in stark contrast to the photon-like model in which the resulting model is almost, but not exactly, a flat normalization shift. This is in agreement with the fact that the NC $\Delta \rightarrow N\gamma$ background spectrally looks similar to the LEE anomalous events and so a flat increase in events is sufficient to reproduce the excess.

Three iterations of D’Agostini’s method are necessary for the electron-like model to converge such that the bias is consistent with zero, while producing a signal statistically equivalent to the observed excess, whereas only two are needed in the case of the photon-like model, primarily because the unfolded solution is spectrally very similar to the Monte Carlo true spectra.

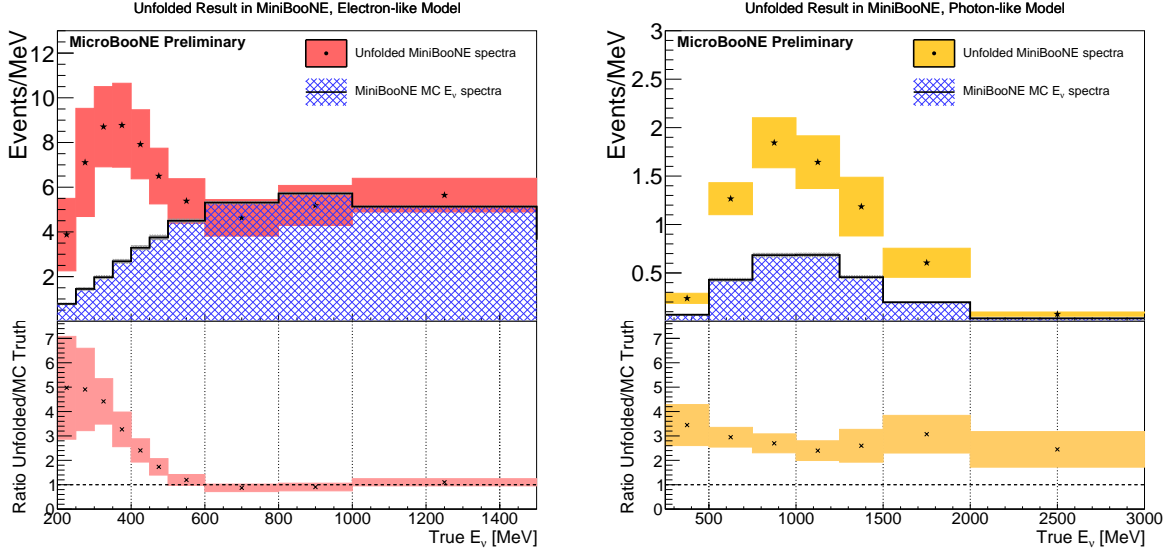


Figure 5: Results of unfolding the MiniBooNE LEE under both the electron-like intrinsic ν_e CC hypothesis (left) and photon-like increased NC resonant Δ production, with subsequent radiative decay hypothesis (right), both obtained using the D’Agostini iterative unfolding algorithm. The unfolded spectra itself, as well as the MiniBooNE Monte Carlo spectrum, t_α , are plotted in both cases indicating the energy dependent increase necessary to account for the observed MiniBooNE LEE, highlighted by the ratio of these which is shown below.

As a cross-check, the results of unfolding the electron-like model using the alternative SVD unfolding approach is shown alongside the D’Agostini’s iterative method in Fig. 6. As can be seen, these distinct algorithms give strikingly similar central value predictions for the unfolded ratio.

As mentioned above, the unfolding cannot be continued below 200 MeV in true neutrino energy as the combined effect of detector, reconstruction and ν_e CCQE analysis selections leads to a 0% MiniBooNE efficiency below this. A 0% efficiency means that any number of true events below this is equally consistent with the MiniBooNE observation, thus any extrapolation below this cutoff energy would have infinite uncertainty and give no additional information. The main reason for this drop in efficiency is a 140 MeV cut applied to the visible energy of the reconstructed EM shower, as well as the lowest energy bin in reconstructed energy being at 200 MeV reconstructed E_ν^{QE} .

The models presented here are the first and prerequisite step in quantifying the level at which MiniBooNE can determine or exclude the origin of the MiniBooNE LEE anomaly. These models, as well as any other hypothesis that one may want to consider, can then be imported into MiniBooNE by rescaling the rate of intrinsic ν_e CC events or rate of NC $\Delta \rightarrow N\gamma$ events in the MiniBooNE Monte Carlo, allowing for their direct inclusion in MiniBooNE analyses.

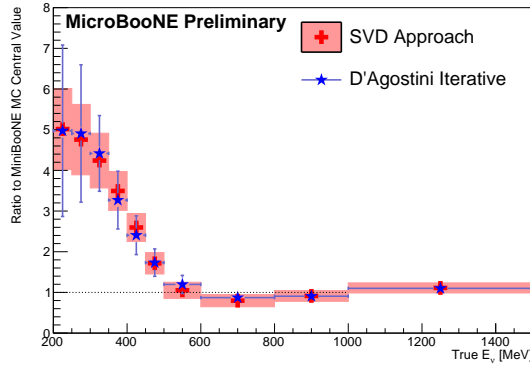


Figure 6: Results of unfolding the MiniBooNE LEE under the intrinsic ν_e CC hypothesis using both the D’Agostini iterative method as well as the alternative SVD unfolding approach.

References

- [1] A. A. Aguilar-Arevalo et al. Improved search for $\bar{\nu}_\mu \rightarrow \bar{\nu}_e$ oscillations in the miniboone experiment. *Phys. Rev. Lett.*, 110:161801, 2013.
- [2] A. Aguilar-Arevalo et al. Evidence for neutrino oscillations from the observation of anti-neutrino(electron) appearance in a anti-neutrino(muon) beam. *Phys. Rev.*, D64:112007, 2001.
- [3] K. N. Abazajian et al. Light Sterile Neutrinos: A White Paper. 2012.
- [4] A. A. Aguilar-Arevalo et al. Observation of a Significant Excess of Electron-Like Events in the Mini-BooNE Short-Baseline Neutrino Experiment. 2018.
- [5] R. Acciarri et al. Design and Construction of the MicroBooNE Detector. *JINST*, 12(02):P02017, 2017.
- [6] G. Karagiorgi B. Murrells, M. Ross-Lonergan. The microboone search for single photon events. *Micro-BooNE Public-Note 1041*.
- [7] T. Wongjirad A. hourlier, K. Terao. First deep learning based event reconstruction for low-energy excess searches with microboone. *MICROBOONE-NOTE-1042-PUB*.
- [8] R. Soleti. Electron-neutrino selection and reconstruction in the microboone lartpc using the pandora multi-algorithm pattern recognition. *MICROBOONE-NOTE-1038-PUB*.
- [9] B. Russel and M.Mooney. Tomographic event reconstruction with microboone data. *MICROBOONE-NOTE-1040-PUB*.
- [10] H. Cramér. *Mathematical Methods of Statistics*. Princeton Mathematical Series. Princeton University Press, 1999.
- [11] C. Radhakrishna Rao. *Information and the Accuracy Attainable in the Estimation of Statistical Parameters*, pages 235–247. Springer New York, New York, NY, 1992.
- [12] G. D’Agostini. A Multidimensional unfolding method based on Bayes’ theorem. *Nucl. Instrum. Meth.*, A362:487–498, 1995.
- [13] Andreas Hocker and Vakhtang Kartvelishvili. SVD approach to data unfolding. *Nucl. Instrum. Meth.*, A372:469–481, 1996.

- [14] William Hadley Richardson. Bayesian-based iterative method of image restoration*. *J. Opt. Soc. Am.*, 62(1):55–59, Jan 1972.
- [15] L. B. Lucy. An iterative technique for the rectification of observed distributions. 79:745, June 1974.
- [16] Y. Vardi, L. A. Shepp, and L. Kaufman. A statistical model for positron emission tomography. *Journal of the American Statistical Association*, 80(389):8–20, 1985.
- [17] Tim Adye. Unfolding algorithms and tests using RooUnfold. In *Proceedings, PHYSTAT 2011 Workshop on Statistical Issues Related to Discovery Claims in Search Experiments and Unfolding, CERN, Geneva, Switzerland 17-20 January 2011*, pages 313–318, Geneva, 2011. CERN, CERN.
- [18] Tim Adye. Corrected error calculation for iterative bayesian unfolding. http://hepunix.rl.ac.uk/~adye/software/unfold/bayes_errors.pdf.
- [19] A. N. Tikhonov. pages 1035–1038. Soviet Mathematics, 1963.